

# Peak effect and square-to-rhombic vortex lattice transition in $\text{La}_{2-x}\text{Sr}_x\text{CuO}_4$

B. Rosenstein,\* B. Ya. Shapiro,† I. Shapiro, Y. Bruckental, A. Shaulov, and Y. Yeshurun  
*Department of Physics, Bar Ilan University, Ramat Gan 52100, Israel*

(Received 27 June 2005; published 17 October 2005)

A theory of structural phase transition of the vortex lattice in tetragonal superconductors is constructed based on the self consistent harmonic approximation for lattice anharmonicities, within the fourfold-symmetric generalization of the London model. Thermal fluctuations on the mesoscopic scale are strong enough to affect the location of the square to rhomb transition line in the  $T$ - $H$  plane. We find that the slope of the transition line is generally negative: thermal fluctuations favor the more symmetric square lattice. The calculated transition line is concave, and fits the experimental line deduced in *LaSCO* crystals from the onset of the second magnetization peak. Near the transition line the “squash” modulus  $C_{sq}=2(C_{11}+C_{12})-C_{66}$  is softened leading to enhancement of the critical current, born out in the experiment as a second magnetization peak.

DOI: [10.1103/PhysRevB.72.144512](https://doi.org/10.1103/PhysRevB.72.144512)

PACS number(s): 74.20.De, 74.25.Ha, 74.25.Qt

## I. INTRODUCTION

Vortex systems in type II superconductors have become a convenient object of choice in studying the complex interplay between interactions, thermal fluctuations and disorder. When thermal fluctuations and disorder can be neglected the system organizes itself into a vortex lattice. However, both disorder and thermal fluctuations tend to destroy it, creating a “vortex glass” or a “vortex liquid.” While the melting line separates the crystalline and liquid phases (dashed line on Fig. 1),<sup>1</sup> the line defined by the second magnetization peak<sup>2</sup> (dash-dotted line on Fig. 1) separates the crystalline solid (Bragg glass) from the vortex glass phase.<sup>3</sup> Originally, it was widely believed that these two lines are not related and intersect at a point. Recently, however, it became evident experimentally<sup>4–6</sup> and theoretically<sup>7</sup> that the two lines constitute just two segments of a single “unified” order-disorder (OD) phase transition line.<sup>5</sup> In  $\text{Bi}_2\text{Sr}_2\text{CaCu}_2\text{O}_{8+\delta}$  (*BSCCO*) the line in the  $B$ - $T$  plane defined by the onset of the second magnetization peak (SMP) exhibits the (positive slope) “inverse melting” phenomenon.<sup>4</sup> At the maximum there appears a Kauzmann point (a noncritical point in which the entropies of the two phases are equal). Similar behavior was found in  $\text{YBa}_2\text{Cu}_3\text{O}_{7-\delta}$  (*YBCO*).<sup>6</sup>

Apparently, however, the high  $T_c$  superconductor  $\text{La}_{2-x}\text{Sr}_x\text{CuO}_4$  (*LaSCO*) constitutes an exception. The melting line and the SMP line clearly cannot be considered as segments of a single OD line. First, unlike in *BSCCO* and *YBCO*, the SMP line in *LaSCO* has a negative slope<sup>8,9</sup> and therefore cannot be considered as the inverse melting section of the OD line. Second, very recently, Divakar *et al.*,<sup>10</sup> using muon spin rotation ( $\mu\text{SR}$ ) and small angle neutron scattering (SANS), demonstrated that the melting line in *LaSCO* continues to the low temperature region as an inverse melting line, similar to that observed in *BSCCO* and *YBCO*, and that the SMP line lies entirely inside the Bragg glass region. Generally, the peak effect is caused by softening of the vortex matter due to a phase transition. A question arises: what transition is signified by the SMP in *LaSCO*?

It has been known for a long time that in certain anisotropic low  $T_c$  superconductors (borocarbides  $\text{YNi}_2\text{B}_2\text{C}$ ,<sup>11</sup>

$\text{LuNi}_2\text{B}_2\text{C}$ ,<sup>12,13</sup>  $\text{Nb}$ ,<sup>14</sup> and  $\text{V}_3\text{Si}$ )<sup>15</sup> the vortex solid phase undergoes structural phase transformations (SPT). In addition it was recently firmly established that the high  $T_c$  superconductor *YBCO* has both square<sup>16</sup> and rhombic<sup>17</sup> phases, although it is difficult to directly observe the transition line using conventional techniques such as decoration, SANS or  $\mu\text{SR}$ . In overdoped *LaSCO*, at low temperatures, the square and rhombic lattices were observed using SANS by Gilardi *et al.*<sup>18</sup> Theoretically, it was shown that a structural phase transition leads to a peak effect due to softening of certain elastic modulus<sup>19</sup> identified in the square-to-rhomb transition as the “squash” modulus.<sup>20</sup> It is natural therefore to conjecture that the SMP line of *LaSCO* signifies a structural phase transition. To test this conjecture we revisited the theory of the rhomb-to-square transition in the presence of strong thermal fluctuations in the London limit, and compared the results with experimental data measured in  $\text{La}_{2-x}\text{Sr}_x\text{CuO}_4$  samples with different doping concentrations  $x$ .

The square-to-rhomb transition is by far the simplest possible structural phase transition. Since the  $z$  direction translation symmetry is not broken in the vortex lattice (and fluctuations along this direction in anisotropic systems like *LaSCO* are highly suppressed), the transition is effectively two dimensional. The broken symmetry is just  $Z_4 \rightarrow Z_2$  (rotations of  $90^\circ$  to rotations of  $180^\circ$ , the inversion symmetry

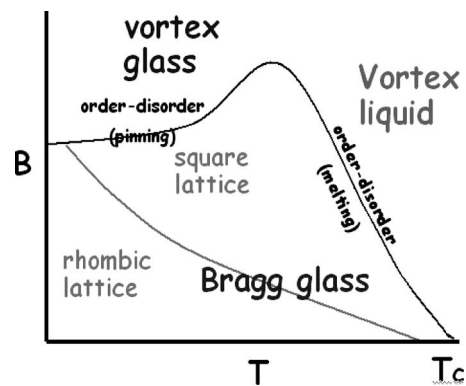


FIG. 1. The vortex matter phase diagram of a tetragonal high  $T_c$  superconductor *LaSCO*.

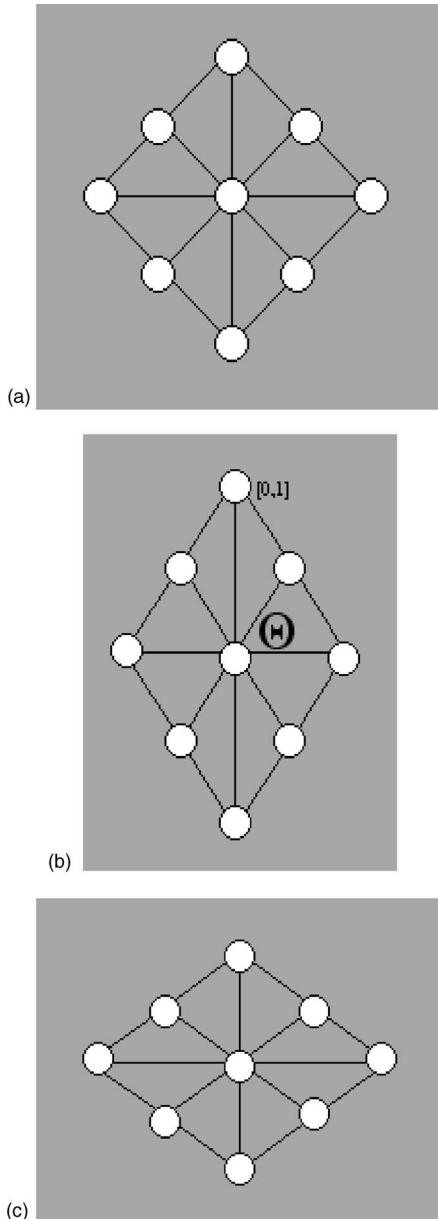


FIG. 2. Two possible vortex lattice structures in a fourfold symmetric superconductor: (a) Square vortex lattice oriented along the  $[110]$  crystallographic axis of atomic lattice; (b) and (c) Two rhombic structures in the low temperature vortex phase: (b) is rotated by  $90^\circ$  with respect to (c).

remains unbroken), namely the same breaking pattern  $Z_2 \rightarrow 1$  as in the Ising model. In the less symmetric phase there are two rhombic lattices differing by a  $90^\circ$  rotation [Figs. 2(a) and 2(b)], while in the more symmetric phase, i.e., the square lattice [see Fig. 2(c)], the vector between two closest vortices may be either parallel to the crystallographic axis  $a$  of the atomic lattice, or rotated by  $45^\circ$  with respect to it. Physically, the coupling between the crystal lattice and the vortex lattice in a fourfold symmetric superconductor such as *LaSCO* (we ignore the very small deviation from the tetragonal symmetry) or certain low  $T_c$  material (such as borocarbide  $RNi_2B_2C$ ,  $R=Y, Lu, Er, V_3Si$ ) originates in two somewhat related anisotropies on a microscopic scale.<sup>21–23</sup> The

first is the Fermi velocity dependence on the angle  $\theta$ :  $v_F(\theta) = v_F[1 + \mu_1 \cos(4\theta)]$ . It is believed that it introduces anisotropy of the inter-vortex interactions largely at low momenta (on the scale  $\lambda$ , where  $\lambda$  is the magnetic penetration depth in the  $ab$  plane), as was extensively studied by Kogan and collaborators<sup>20</sup> in the framework of the nonlocal London theory. The second is the anisotropy of the gap function  $|\Delta(\theta)|^2 = |\Delta_0|^2[1 - \mu_2 \cos(4\theta)]$  (Ref. 23) resulting in the anisotropy of the vortex-vortex interaction on the scale of the coherence length  $\xi$ . This anisotropy is obviously present and perhaps dominant in the  $d$ -wave superconductors due to the nodes in the order parameter. It is this asymmetry which is effectively taken into account in the Ginzburg-Landau approach to the rhomb-to-square structural phase transition<sup>24,25,27</sup> and it is taken into account within the nonlocal London approach as an asymmetric moment cutoff.<sup>20</sup>

In this paper we are primarily interested in the part of the phase diagram  $B \ll H_{c2}(T)$ , where the vortex core size  $\xi$  is much smaller than the distance  $a$  between vortices. At first glance, the structural phase transition in such a system, even at finite temperature (below the melting temperature of course), is driven by interactions on scales smaller than  $c_L a_0$ , where  $c_L \sim 0.1$  is the Lindemann constant, and consequently have nothing to do with anisotropy of the vortex core. However, it was claimed in a recent theory of thermal fluctuations<sup>28</sup> that the core anisotropy is crucial. Thus the problem should be considered from a more fundamental approach. A standard approach to the crystal structure of point-like (or line-like) objects at finite temperature requires a sufficiently comprehensive account of the lattice anharmonicity.<sup>29</sup> The simplest version of such a theory takes into account the interacting phonon excitations self-consistently [the self-consistent harmonic approximation (SCHA)]. Such, and even more refined in certain respects, methods were applied to the vortex physics in the context of the 2D melting in Ref. 30. In the present study we show that the SCHA is sufficient to describe the rhomb-to-square transition line.

We parametrize the asymmetry on the scale  $\lambda$  by a single parameter and obtain a structural phase transition line with a negative slope in the  $B$ - $T$  plane, using the microscopic derivation of the vortex-vortex interaction for a  $d$ -wave superconductor by Yang.<sup>33</sup> In our theory, unlike the preceding ones,<sup>28</sup> no cutoff is required. The results of our theory compare well with experimental data in *LaSCO* in a wide range of doping.

The paper is organized as follows. The choice of the model and the phase transition at zero temperature are discussed in Secs. II and III, respectively. The SCHA for square lattice and fourfold symmetric potential and the variational method are developed in Sec. IV. In Sec. V we compare experiments on *LaSCO* with our theory. Discussion of the general symmetry properties of the transition and comparison with other theories are the subjects of Sec. VI.

## II. THE FOUR-FOLD SYMMETRIC POTENTIAL FOR A $d$ -WAVE SUPERCONDUCTOR

For a strongly type II superconductor ( $\kappa \equiv \lambda/\xi \gg 1$ ), isotropic in the  $ab$  plane, the potential of the interaction be-

tween straight line vortices at zero temperature is known to be well approximated by Ref. 34:

$$V(r_{ab}) = \frac{\Phi_0^2}{8\pi^2\lambda^2} [K_0(r_{ab}/\lambda) - K_0(r_{ab}/\xi)], \quad (1)$$

where  $r_{ab}$  is the distance between the vortices. The repulsive part of this potential is due to the long range magnetic interactions, while the attractive part is due to the vortex cores overlap. Note that despite the fact that both terms diverge for  $r_{ab} \rightarrow 0$ , the potential remains finite. Initially, we neglect variations of the penetration depth  $\lambda$  and the coherence length  $\xi$  due to thermal fluctuation on the microscopic scale and therefore we limit ourselves to temperatures far from  $T_c$ . (In Sec. IV C we extend the discussion to the region close to  $T_c$ .) The potential  $V$  is therefore temperature independent.

The same formula applies to layered superconductors like *LaSCO* which are strongly anisotropic with respect to direction  $c$ . Thermal fluctuation in a layers of width  $L_c$  should be considered and the weak coupling between layers ignored. The two dimensional Fourier transform of the potential given in Eq. (1) reads:

$$v(q^2) = L_c \frac{\Phi_0^2}{4\pi} \left( \frac{1}{1+bq^2} - \frac{1}{\kappa^2 + bq^2} \right), \quad (2)$$

where we use  $a_{\square} = \sqrt{\Phi_0/B}$  as a unit of length by writing  $q \rightarrow qa_{\square}/2\pi$ , and

$$b \equiv \frac{(2\pi\lambda)^2 B}{\Phi_0} = \frac{\pi B}{H_{c1}} \ln \kappa \quad (3)$$

is a dimensionless magnetic field. The potential decreases as  $1/q^4$  in the ultraviolet. Commonly, the potential of Eq. (2) is approximated by a simpler cutoff form  $1/(1+bq^2) \times \exp(-b/(\kappa^2)q^2)$ .<sup>20,28,35</sup>

In a fourfold symmetric superconductor there are asymmetries at various scales. The vortex-vortex interaction potential at distances larger than the core size was derived from a microscopic model of the  $d$ -wave superconductor by Yang.<sup>33</sup> Here we parametrize Yang's potential  $w$  by the single in-plane anisotropy parameter  $\eta$ :

$$w(q_x, q_y) = \left[ 1 + \eta \left( \frac{\beta h}{1 + \beta g} \right)^2 \right] v(g), \quad (4)$$

where  $g = q_x^2 + q_y^2$ ,  $h = q_x^2 - q_y^2$ . This potential, which does not diverge for both large and small momenta, differs from the one of the nonlocal linearized London model<sup>20,28</sup>

$$\frac{1}{1 + bg + b^2 t_1 g^2 + b^2 t_2 q_x^2 q_y^2} \exp\left(-\frac{b}{\kappa^2 g}\right), \quad (5)$$

in that nonlinear corrections to Gor'kov equations are taken into account. Expanding Eq. (5) to the first order in the small parameter  $t_2$ , one obtains a term similar to Eq. (4), however it is generally impossible to obtain the exponentially decreasing cutoff from first principles. The potential's dependence on the single parameter  $\eta$  is obviously not the most general one, but it allows us to qualitatively model the physics of the structural phase transitions.

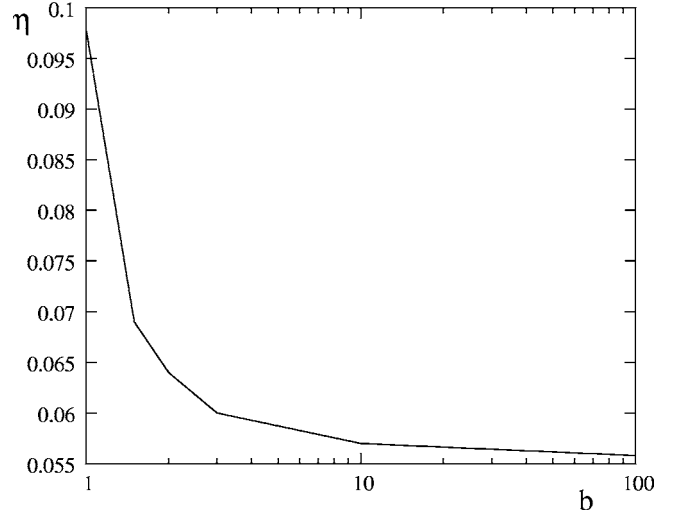


FIG. 3. Transition line at zero temperature separating the rhombic vortex lattice phase from the square vortex lattice phase. The dependence of critical four-fold anisotropy parameter  $\eta_c$  on  $b$ , where  $b$  is the dimensional magnetic field  $b = 4\pi^2 B \lambda^2 / \Phi_0$ .

### III. STRUCTURAL TRANSITION AT ZERO TEMPERATURE

#### A. Lattice energy

At zero temperature the vortex lattice structure is determined by minimization of the lattice sum over the reciprocal lattice of arbitrary symmetry:

$$E_0 = \frac{1}{2} \sum_{nm} w(\mathbf{G}_{nm}), \quad (6)$$

where  $\mathbf{G}_{nm}$  are the reciprocal lattice vectors. We restrict ourselves to rhombic lattices with the opening angle  $2\Theta$ . It turns out (see also Ref. 23) that for a positive asymmetry parameter  $\eta$ , the rhombic lattices oriented along the crystallographic axis (110) [see Fig. 2(b)] with

$$\mathbf{G}_{nm} = n\mathbf{q}_1 + m\mathbf{q}_2; \quad \mathbf{q}_1 = \frac{1}{\sqrt{2 \tan \Theta}} (1, \tan \Theta);$$

$$\mathbf{q}_2 = \frac{1}{\sqrt{2 \tan \Theta}} (1, -\tan \Theta)$$

have energy lower than other lattice structures [rhombic oriented along (100) or oblique].

Calculating the  $E_0(\Theta)$  sum for the rhombic lattices in the whole range of angles ( $\Theta = 45^\circ - 60^\circ$ ), one obtains that above a certain critical asymmetry  $\eta_c(b)$  the square lattice has lower energy than the rhombic, while below it one of the rhombic structures either Fig. 2(b) or Fig. 2(c) is preferred. The dependence of  $\eta_c$  on  $b$  is presented in Fig. 3. When calculating the angle dependence of the lattice energy, it becomes clear that the transition is of a second order type with mean field critical exponents. Similar results have been found with a different fourfold symmetric potential in the London limit<sup>20</sup> and within the Ginzburg-Landau model.<sup>24,25</sup>

At finite temperature (well below the melting point) thermodynamics is dominated by the long wavelength phonons.

### B. Phonons and SPT

In this subsection we determine the spectrum of phonons and its relation to the rhomb-to-square structural transformation. A macroscopic manifestation of the structural phase transition is the softening of the elastic squash modulus

$$C_{sq} = 2(C_{11} + C_{12}) - C_{66} \quad (7)$$

at the transition point.<sup>20</sup> We consider a simplified model of a vortex as an elastic line with an effective stiff segments of the length  $L_z$ . The length is determined by comparison of the tilt energy to the energy of the softest modes (the squash modes)<sup>26</sup> and is estimated in Sec. V.

The softening is reflected in the reduction of the sound velocity of acoustic phonons along several directions. To see this let us consider the energy  $E[\mathbf{u}_a]$  of displacements of vortices  $\mathbf{u}_a$  from their equilibrium square lattice positions  $\mathbf{R}_a$

$$E[\mathbf{u}_a] = \frac{1}{2} \sum_{a \neq b} w(\mathbf{R}_a - \mathbf{R}_b + \mathbf{u}_a - \mathbf{u}_b). \quad (8)$$

Since the symmetric phase is aligned along the (110) crystallographic axis, it is natural to use the coordinate system rotated in this direction. In this coordinate system the potential (4) has the form:

$$w(q_x, q_y) = \left[ 1 + \eta \left( \frac{2bq_x q_y}{1 + bg} \right)^2 \right] v(g). \quad (9)$$

The corresponding reciprocal lattice vectors are integers  $\mathbf{G}=(n, m)$ . Expanding Eq. (8) to the second order in the small displacement and switching to the Fourier harmonics on the Brillouin zone of the square lattice  $q_x, q_y \in [-\frac{1}{2}, \frac{1}{2}]$ ,  $\mathbf{u}_a = \sum_{\mathbf{BZ}} u_{\mathbf{q}}^\alpha \exp(i\mathbf{q}\mathbf{R}_a)$ , one obtains  $E[\mathbf{u}_q] \approx E_0 + E_2[\mathbf{u}_q]$  where

$$E_2[\mathbf{u}_q] = \frac{1}{2} \sum_{\mathbf{BZ}} \Lambda_{\alpha\beta}(q) u_{\mathbf{q}}^\alpha u_{-\mathbf{q}}^\beta. \quad (10)$$

Elastic moduli are given by the expansion of  $\Lambda$  to the second order in  $q$ :  $\Lambda_{\alpha\beta}(q) = C^{\alpha\beta\gamma\delta} q_\gamma q_\delta$ . The only nonzero moduli in the fourfold symmetry case, namely, compression  $C_{11}$ , shear  $C_{66}$ , and squash  $C_{sq}$  moduli presented in Fig. 4. Note that  $C_{sq}$  vanishes for  $\eta \rightarrow \eta_c$ , while the rest are constant. The stability conditions (positively definite quadratic form  $E_2[\mathbf{u}_q]$ ) for the square lattice are  $4(C_{11} + C_{66}) > C_{sq} > 0$  and  $C_{66} > 0$ . It is expected that increasing temperature will shift the structural transition temperature towards lower fields. To incorporate the temperature effects on the phase transition, the standard phonon perturbation theory is not sufficient and certain resummations are required. The simplest one is the self-consistent harmonic approximation.

## IV. SELF CONSISTENT HARMONIC APPROXIMATION FOR A FOURFOLD SYMMETRIC INTERACTIONS

### A. General SCHA

Generally thermal excitations at temperature  $T$  are taken into account by calculating the statistical sum

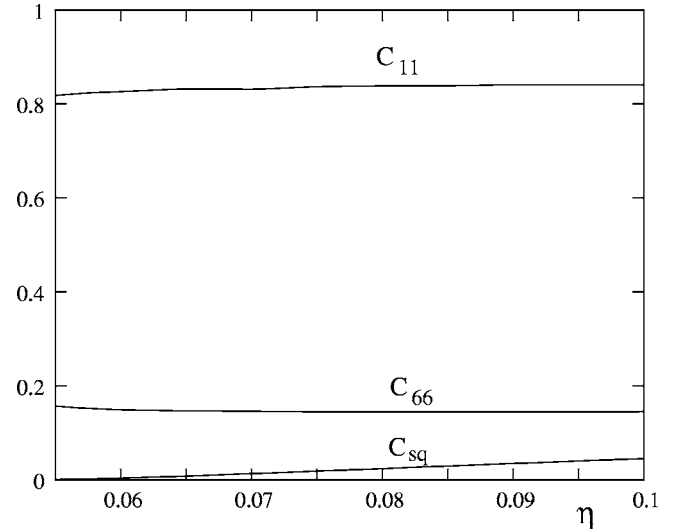


FIG. 4. The compression, shear and squash elastic moduli in the square lattice phase as function on the fourfold anisotropy parameter  $\eta$  at zero temperature.

$$Z = \int \mathcal{D}u e^{-H[\mathbf{u}_q]/T}, \quad \mathcal{D}u = \prod_{\mathbf{q} \in \text{BZ}} d^2 u_{\mathbf{q}}. \quad (11)$$

To develop a SCHA one has to take into account the interactions between phonons (anharmonicities) to the third and fourth orders in  $u_{\mathbf{q}}^\alpha$ . The third order however will drop out later on (see Ref. 30 for details, although we use a more general Ansatz for the variational correlator) and we just write the quartic term in the expansion:

$$H[\mathbf{u}_q] = E_0 + E_2[\mathbf{u}_q] + E_4[\mathbf{u}_q],$$

$$E_4[\mathbf{u}_q] = \frac{1}{4!} \sum_{\mathbf{k}, \mathbf{l}, \mathbf{m} \in \text{BZ}} \Omega_{\alpha\beta\gamma\delta}(q, l, m) u_{\mathbf{q}}^\alpha u_{\mathbf{l}}^\beta u_{\mathbf{m}}^\gamma u_{-\mathbf{q}-\mathbf{l}-\mathbf{m}}^\delta. \quad (12)$$

In the SCHA scheme, belonging to the broad class of ‘‘Gaussian’’ approximations, one adds and subtracts a quadratic form with variational correlator  $T\Delta_{\alpha\beta}(q)$ .<sup>36</sup> Then the variational part  $\Delta_{\alpha\beta}^{-1}(k) u_{\mathbf{q}}^\alpha u_{-\mathbf{q}}^\beta / 2$  is considered the ‘‘large’’ (or Gaussian) part, while the rest of Hamiltonian is a small perturbation. Therefore it is multiplied by an artificial small parameter  $\varepsilon$ :

$$Z = \int \mathcal{D}u \exp \left[ \varepsilon \left( -\frac{H}{T} + \frac{\Delta_{\alpha\beta}^{-1}(k) u_{\mathbf{q}}^\alpha u_{-\mathbf{q}}^\beta}{2T} \right) \right] \times \exp \left( -\frac{\Delta_{\alpha\beta}^{-1}(k) u_{\mathbf{q}}^\alpha u_{-\mathbf{q}}^\beta}{2T} \right). \quad (13)$$

One subsequently expands to first order in  $\varepsilon$  taking  $\varepsilon \rightarrow 1$  after performing Gaussian integrations over  $u_{\mathbf{q}}^\alpha$ . The Gaussian effective free energy  $Z = \exp\{-f_{eff}\}$  reads:

$$f_{eff} = \frac{E_0}{T} + f_1 + f_2 + f_4, \quad (14)$$

$$f_1 = -\frac{1}{2} \text{Tr} \sum_{\mathbf{q}} \ln(2T\pi\Delta_{\alpha\beta}(q)), \quad (15)$$

$$f_2 = \frac{1}{2} \sum_{\mathbf{q}} \Lambda_{\alpha\beta}(q)\Delta_{\alpha\beta}(q), \quad (16)$$

$$f_4 = \frac{3T}{4!} \sum_{\mathbf{q}, \mathbf{l}} \Omega_{\alpha\beta\gamma\delta}(q, -q, \mathbf{l}, -\mathbf{l}) \Delta_{\alpha\beta}(q) \Delta_{\gamma\delta}(\mathbf{l}). \quad (17)$$

This should be minimized with respect to the variational function  $\Delta_{\alpha\beta}(q)$ . Explicit evaluation of the coefficient functions  $\Lambda_{\alpha\beta}(q)$  and  $\Omega_{\alpha\beta\gamma\delta}(q, -q, \mathbf{l}, -\mathbf{l})$  results in (up to unimportant terms independent of  $\Delta_{\alpha\beta}$ ):

$$f_2 = \sum_{\mathbf{q}} \left\{ w(q-G) \left[ (q-G)^x (q-G)^x \Delta^{xx}(q) + (q-G)^y (q-G)^y \Delta^{yy}(q) \right] + 2(q-G)^x (q-G)^y \Delta^{xy}(q) \right\} - w(G) \left[ (G)^x (G)^x \Delta^{xx}(q) + (G)^y (G)^y \Delta^{yy}(q) + 2(G)^x (G)^y \Delta^{xy}(q) \right] \quad (18)$$

and

$$f_4 = \frac{T}{2} \sum_{\mathbf{q}_1} \sum_{\mathbf{q}_2} [A + B - 2C], \quad (19)$$

where

$$\begin{aligned} A &= w(G) [G^x G^x \Delta^{xx}(q_1) + G^y G^y \Delta^{yy}(q_1) + 2G^x G^y \Delta^{xy}(q_1)] \\ &\quad [G^x G^x \Delta^{xx}(q_2) + G^y G^y \Delta^{yy}(q_2) + 2G^x G^y \Delta^{xy}(q_2)] \\ B &= w(q_1 + q_2 + G) \left[ (q_1 + q_2 + G)^x (q_1 + q_2 + G)^x \Delta^{xx}(q_1) \right. \\ &\quad \left. + (q_1 + q_2 + G)^y (q_1 + q_2 + G)^y \Delta^{yy}(q_1) \right. \\ &\quad \left. + 2(q_1 + q_2 + G)^x (q_1 + q_2 + G)^y \Delta^{xy}(q_1) \right] \\ &\quad \left[ (q_1 + q_2 + G)^x (q_1 + q_2 + G)^x \Delta^{xx}(q_2) + \right. \\ &\quad \left. (q_1 + q_2 + G)^y (q_1 + q_2 + G)^y \Delta^{yy}(q_2) + 2(q_1 + q_2 + G)^x (q_1 + q_2 + G)^y \Delta^{xy}(q_2) \right], \\ C &= w(q_1 + G) \left[ (q_1 + G)^x (q_1 + G)^x \Delta^{xx}(q_1) \right. \\ &\quad \left. + (q_1 + G)^y (q_1 + G)^y \Delta^{yy}(q_1) + 2(q_1 + G)^x (q_1 + G)^y \Delta^{xy}(q_1) \right] \\ &\quad \left[ (q_1 + G)^x (q_1 + G)^x \Delta^{xx}(q_2) + (q_1 + G)^y (q_1 + G)^y \Delta^{yy}(q_2) \right. \\ &\quad \left. + 2(q_1 + G)^x (q_1 + G)^y \Delta^{xy}(q_2) \right]. \end{aligned} \quad (20)$$

It will be sufficient for our purposes to consider a much simpler Ansatz when instead of three functions of two variables  $\Delta^{xx}(\mathbf{q}), \Delta^{yy}(\mathbf{q}), \Delta^{xy}(\mathbf{q})$  we will minimize just over three variables representing elastic moduli of the lattice. We describe the Ansatz in the next subsection.

### B. The linear dispersion approximation

It is well established that near the second order square to rhomb SPT the relevant degrees of freedom are the long wavelength ones. Therefore one can expand the self-consistent dispersion function (in rotated coordinate system) in small momenta

$$\Phi_{\alpha\beta} = (\Delta_{\alpha\beta})^{-1} = c^{\alpha\beta\gamma\delta} q_\gamma q_\delta \quad (21)$$

or in components

$$\begin{aligned} \Phi_{xx} &= c_{11} q_x^2 + c_{66} q_y^2; & \Phi_{xy} &= c q_x q_y; & \Phi_{yy} &= c_{11} q_y^2 + c_{66} q_x^2 \\ c &= c_{11} - \frac{c_{sq}}{2} + c_{66} \end{aligned} \quad (22)$$

where  $c_{sq}$  is defined as in Eq. (7). It was checked *a posteriori* that this approximation is extremely accurate everywhere in the Brillouin zone for parameters of interest. The relation between these variational parameters and elastic moduli in the crystallographic axes coordinate system is

$$\begin{aligned} c_{11} &= C_{11} + C_{66} - C_{sq}/4, \\ c_{66} &= C_{sq}/4, \quad c_{sq} = 4C_{66}. \end{aligned} \quad (23)$$

We therefore parametrize  $\Delta_{\alpha\beta}$  by these three moduli.

It is crucially important to have the correct infrared asymptotics of the correlators. Note that this Ansatz is very different from the usual simplification made within SCHA.<sup>30</sup> The later in the configuration space reads:

$$\langle (u_a^\alpha - u_b^\alpha)(u_a^\beta - u_b^\beta) \rangle \approx \delta^{\alpha\beta} \langle u_a^2 \rangle. \quad (24)$$

In momentum space it translates into

$$\sum_q \Delta^{\alpha\beta}(q) \cos(\mathbf{q}\mathbf{R}_{ab}) \ll \sum_q \Delta^{\alpha\beta}(q), \quad (25)$$

which is doubtful when a soft mode appears. In order to discuss the second order phase transition, soft modes are essential.

### C. Minimization of the variational free energy

In order to find the structural phase transition line one tries to find the minimum of the variational free energy Eq. (14) for the square lattice with respect to the variational parameters  $c_{11}$ ,  $c_{66}$ , and  $c_{sq}$  in the range of stability discussed in Sec. II. Values of external parameters  $B$ ,  $T$ , etc. for which the stability conditions are not obeyed, namely  $C_{sq} < 0$ , the transition to the rhombic phase takes place. Now we return to the evaluation of the integrals over  $q$  of the variational free energy Eq. (14) as a function of the variables  $c_{11}$ ,  $c_{66}$ , and  $c_{sq}$ . The first term has the form

$$f_1 = \frac{1}{2} \{ \ln(c_{11}^2 c_{66}) + e_1(r) \}, \quad (26)$$

where

$$e_1(r) = \int_{-1/2}^{1/2} dq_x dq_y \ln \left( \frac{\det \Phi}{c_{11}^2} \right) = \ln \left( \frac{r+2}{16} \right) - 6 + \pi r_- \\ + r_+ \tan^{-1} \left( \frac{2r_-}{r_+ - 1} \right) + r_- \tan^{-1} \left( \frac{2r_+}{r_- - 1} \right) \quad (27)$$

and the dimensionless ratios of moduli are defined by:

$$r = \frac{c_{11}^2 + c_{66}^2 - c^2}{c_{11} c_{66}}, \quad r_{\pm} = \sqrt{\frac{r}{2} \pm \sqrt{\frac{r^2}{4} - 1}}. \quad (28)$$

The second contribution is

$$f_2 = \frac{1}{2c_{11}} e_2(c_{sq}/c_{11}, c_{66}/c_{11}) \quad (29)$$

$$e_2(c_{sq}/c_{11}, c_{66}/c_{11}) = v_1 b_1 + v_2 b_2 + v_3 b_3, \quad (30)$$

where the integrals appearing in Eq. (18) and (20)

$$b_1 = \int_{-1/2}^{1/2} dq_x dq_y \frac{c_{11} q_x^2 (c_{11} q_x^2 + c_{66} q_y^2)}{\det \Phi} \\ = \frac{c_{11}}{2c_{66}} + \left( 1 - \frac{rc_{11}}{2c_{66}} \right) I(r),$$

$$b_2 = \int_{-1/2}^{1/2} dq_x dq_y \frac{c_{11} q_y^2 (c_{11} q_x^2 + c_{66} q_y^2)}{\det \Phi} = \frac{1}{2} + \left( \frac{c_{11}}{c_{66}} - \frac{r}{2} \right) I(r),$$

$$b_3 = \int_{-1/2}^{1/2} dq_x dq_y \frac{c_{11} c_{sq} q_x^2 q_y^2}{\det \Phi} = \frac{c}{c_{66}} I(r), \quad (31)$$

are expressed via a function of  $r$

$$I(r) = \frac{c_{11} c_{66}}{c} \int_{-1/2}^{1/2} dq_x dq_y \frac{q_x^2 q_y^2}{\det \Phi} \\ = \left[ r_+ \tan^{-1} \left( \frac{1}{r_+} \right) - r_- \tan^{-1} \left( \frac{1}{r_-} \right) \right] (r^2 - 4)^{-1/2}. \quad (32)$$

The coefficients  $v_i$  depend on the potential and are given in the Appendix. The last contribution to the free energy reads:

$$f_4 = \frac{\tau}{2c_{11}^2} e_4(c_{sq}/c_{11}, c_{66}/c_{11}) \quad (33)$$

$$e_4(c_{sq}/c_{11}, c_{66}/c_{11}) = v_{11} b_1^2 + v_{22} b_2^2 + v_{33} b_3^2 + 2v_{12} b_1 b_2 \\ + 2v_{13} b_1 b_3 + 2v_{23} b_2 b_3, \quad (34)$$

where the dimensionless temperature

$$\tau = \frac{4\pi T}{L_z \Phi_0 B} \quad (35)$$

was introduced.

The free energy Eq. (14) can now be minimized explicitly with respect to  $c_{11}$ :

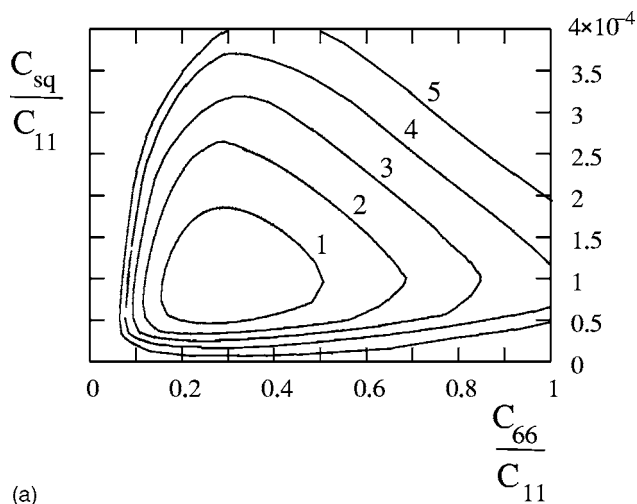
$$c_{11} = \frac{1}{4} [e_2 + \sqrt{e_2^2 + 16\tau e_4}], \quad (36)$$

leaving us with numerical minimization with respect to the two remaining parameters: ratios of elastic moduli. As an example of this procedure we present in Fig. 5(a) the free energy for  $\eta=0.03$ ,  $\tau b=0.2 \times 10^{-4}$ ,  $b=20$  as a function of  $C_{sq}/C_{11}$  and  $C_{66}/C_{11}$ . The minimum appears at  $C_{sq}/C_{11} = 10^{-5}$ ,  $C_{66}/C_{11} = 0.3$ . The small value of the squash modulus implies that this point is very close to the loss of the square lattice stability line. In Fig. 5(b) we slightly lowered the temperature and as a result the minimum disappeared. One clearly observes that the squash modulus vanishes at the point where the square lattice becomes unstable. Figure 6(a) presents the squash modulus  $C_{sq}$  (in the original coordinate system, namely tied to crystallographic axes) as a function of the fourfold asymmetry parameter  $\eta$ , at temperatures  $T=0$ ,  $T_c/6$ , and  $T_c/3$  (magnetic field is  $b=10$  and  $\kappa=35$ ). The temperature dependence of  $C_{sq}$  for  $\eta=0.03$  and two different magnetic fields are shown in Fig. 6(b) (curve 1 corresponds to  $b=10$ , and curve 2 to  $b=20$ ). It can be fitted precisely in the whole region shown in the figure by the power law:

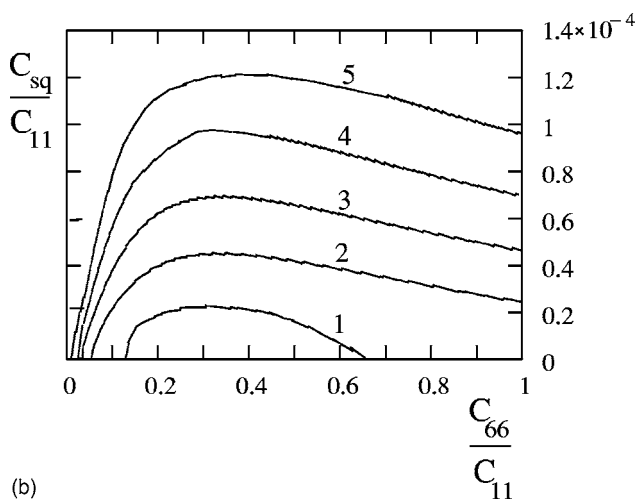
$$C_{sq} = \text{const}(T - T_{ST})^\mu \quad (37)$$

where  $T_{ST}$  is the temperature of the square-to-rhomb transition and the critical exponent  $\mu = \frac{3}{2}$ . A typical vortex lattice phase diagram in the  $b$ - $t$  plane is presented in Fig. 7 for  $\kappa = 75$ , and  $\eta = 0.003, 0.0165, 0.03, 0.05$ . The transition line is fitted accurately by the following function

$$b = g(\Theta) = \frac{A_0(\eta, \kappa)}{\Theta^\nu} [\Theta_0(\eta, \kappa) - \Theta];$$



(a)



(b)

FIG. 5. (a) Free energy as function of variational parameters  $C_{66}/C_{11}$  and  $C_{sq}/C_{11}$  just above the rhomb-to-square transition line [ $\eta=0.03$ ,  $\tau=4\pi T/(L_z\Phi_0 B)$ ,  $\tau=4\times 10^{-5}$ ,  $b=20$ ]. Minimum clearly exists although the “soft” modulus, the squash is very small. (b) Free energy at the transition ( $\eta=0.03$ ,  $\tau=4\times 10^{-5}$ ,  $b=15$ ). The minimum of energy disappears, while the squash modulus vanishes.

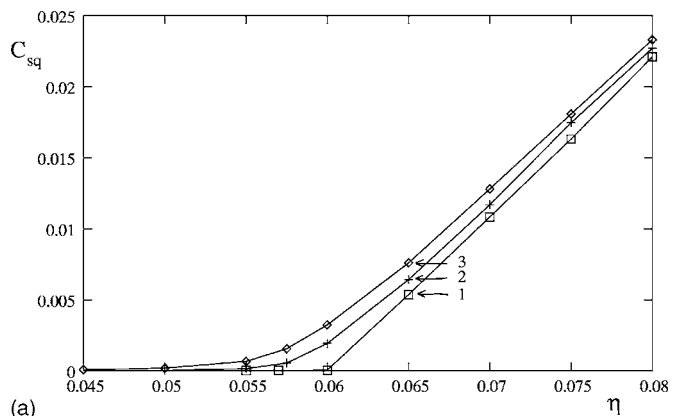
$$\Theta = b\tau \equiv \alpha t; \quad \alpha = 4\pi^3\lambda^2 T_c / L_z \Phi_0^2, \quad (38)$$

where  $t=T/T_c$ . Above the temperature at which  $\Theta=\Theta_0$  the vortex lattice is square for all magnetic fields. At low temperatures the dependence is a power function. In the case presented in Fig. 7 in which  $\kappa=75$  (appropriate to *LaSCO*) the exponent is  $\nu=0.9$  independent of the fourfold anisotropy parameter  $\eta$ .

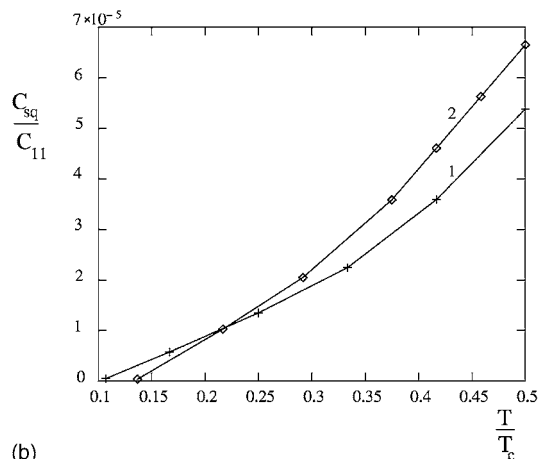
Application of the above theoretical results to experiments in *La<sub>2-x</sub>Sr<sub>x</sub>CuO<sub>4</sub>* sample are discussed next.

## V. EXPERIMENTAL ESTIMATE OF THE FOURFOLD ANISOTROPY PARAMETER IN *LaSCO*

In this section we derive the fourfold anisotropy parameter,  $\eta$ , for *La<sub>2-x</sub>Sr<sub>x</sub>CuO<sub>4</sub>* with different doping concentration  $x$ . The choice of this material was motivated by the following considerations. Since we are interested in a superconductor



(a)



(b)

FIG. 6. (a) The soft modulus  $C_{sq}$  as function of the fourfold anisotropy for three different temperatures  $T=0$ ,  $T_c/6$ , and  $T_c/3$ . Magnetic field is  $b=10$  and  $\kappa=35$ . (b) and (c) The soft modulus  $C_{sq}/C_{11}$  as function of reduced temperature  $T/T_c$  for  $\eta=0.03$  and two magnetic fields  $b=10$  (curve 2) and  $b=20$  (curve 1) where  $\kappa=35$ .

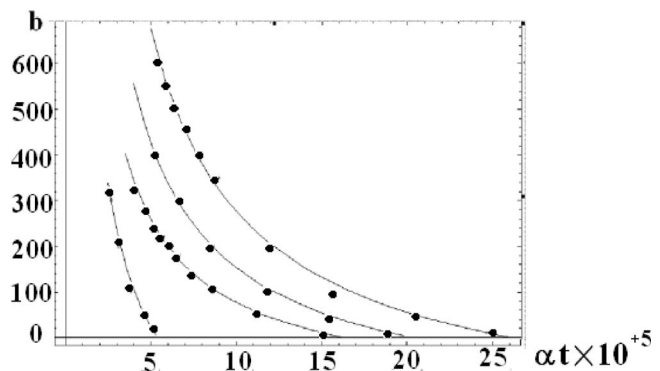


FIG. 7. Location of the square-to-rhomb structural transition on the  $B$ - $T$  plane. The magnetic field  $b=4\pi^2 B \lambda^2 / \Phi_0$  is while the temperature  $\Theta=\alpha T/T_c$ , with material parameter  $\alpha=16\pi^3\lambda^2 T_c / L_z \Phi_0^2$ . The transition lines obtained numerically for  $\kappa=75$  and  $\eta=0.003, 0.0165, 0.03, 0.05$  (circles) (from up to down) is fitted by the function (solid lines)  $b=A_0/\Theta^\nu(\Theta_0-\Theta)$  where  $\nu=0.9$  and does not depend on the fourfold anisotropy parameter  $\eta$ .

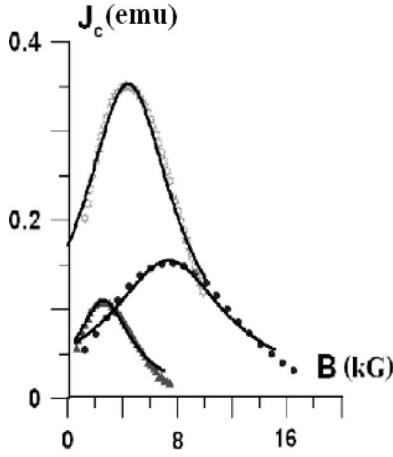


FIG. 8. Critical current as function of magnetic field. Stars correspond to the underdoped sample at  $T=14$  K, circles to the optimally doped sample at  $T=12$  K, while triangles to the overdoped sample at  $T=16$  K. Lines are fits by a function  $J_c$ .

with strong thermal fluctuations, a natural choice is a high  $T_c$  material. In addition, it should be fourfold symmetric. The natural choice would be  $BSCCO$  which is tetragonal. However the OD line in  $BSCCO$  is located too low in the  $B$ - $T$  phase diagram (below 500 G). Since  $YBCO$  has a large in-plane anisotropy, this leaves us with the nearly tetragonal  $LaSCO$  crystals. Three  $La_{2-x}Sr_xCuO_4$  single crystals, with different amount of Sr, were grown<sup>31</sup> by the traveling-solvent-floating-zone method: underdoped (with doping concentration  $x=0.126$ ,  $T_c=32$  K,  $\lambda \approx 2 \times 10^{-5}$ ), optimally doped ( $x=0.154$ ,  $T_c=37$  K,  $\lambda \approx 10^{-5}$ ) and overdoped ( $x=0.194$ ,  $T_c=30$  K,  $\lambda \approx 10^{-5}$ ).<sup>9</sup> Samples of these crystals, were cut into parallelepiped shape with dimensions ( $c \times a \times b$ )  $1.05 \times 1.7 \times 2.3$  mm,  $1.08 \times 0.7 \times 1.17$  mm,  $2.08 \times 0.83 \times 0.96$  mm, respectively. Measurements were performed using a commercial superconducting quantum interference device (SQUID) magnetometer (Quantum Design MPMS-XL) utilizing the RSO technique with 1 cm scans. Magnetization was measured at constant temperature as a function of the external field applied parallel to  $c$  axis and being swept up to 5 T and down to zero in steps of 200 Oe.

The critical current is estimated from the width of the magnetization loop.<sup>32</sup> Examples of the second peak in the critical current as a function of magnetic field are presented in Fig. 8 (stars correspond to the underdoped sample at  $T=14$  K, circles to the optimally doped sample at  $T=12$  K, while triangles to the overdoped sample at  $T=16$  K). The lines describing the SMP for the underdoped sample (line 1 on Fig. 9) and the overdoped sample (line 2 on Fig. 9) in the  $B$ - $T$  plane exhibit negative slopes.

It was predicted that the critical current  $J_c$  for elastic vortex matter in a fourfold symmetric superconductor is proportional to  $(C_{66}C_{sq})^{-1}$ .<sup>19</sup> It should, therefore, diverge at the transition line in an infinite sample due to vanishing of the squash modulus  $C_{sq}$ . The phenomenon is similar to the regular peak effect appearing due to softening of the shear modulus. Finite size and other inhomogeneity effects smooth out the divergence. We fit this dependence phenomenologically

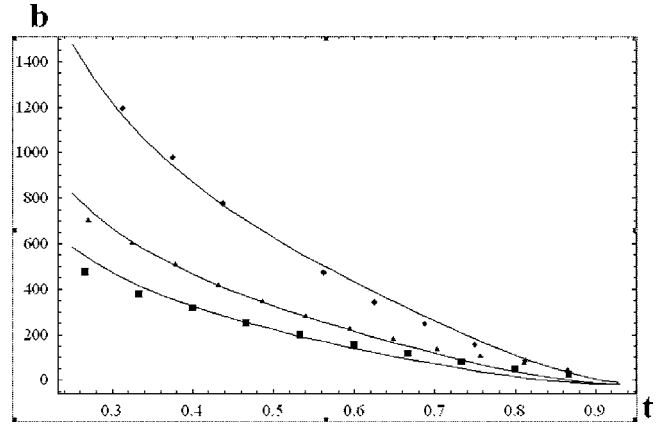


FIG. 9. Comparison of the experimental second magnetization peak line of  $La_{2-x}Sr_xCuO_4$  with the theoretical square-to-rhomb transition line. The squares, stars, and rhombs represent the underdoped, optimally doped and overdoped samples respectively. The theoretical curves (solid lines) are all for  $\kappa=75$  indicate the location of the second magnetization peak for the underdoped sample (diamonds) ( $\eta=0.03$ ,  $\alpha=4 \times 10^{-4}$ ,  $s_1=272$ ,  $s_2=139$ ), for optimally doped sample (triangles) ( $\eta=0.02$ ,  $\alpha=4 \times 10^{-4}$ ,  $s_1=200$ ,  $s_2=123$ ) and for overdoped sample (squares) ( $\eta=0.01$ ,  $\alpha=3.2 \times 10^{-4}$ ,  $s_1=469$ ,  $s_2=165$ ).

to the data of  $J_c$  presented in Fig. 8, using the dependence of the squash modulus near criticality in the form

$$J_c(B) \propto M_{up} - M_{down} = \frac{a}{[(B - B_{ST})^2 + (\Delta B)^2]^{p/2}}, \quad (39)$$

where  $\Delta B$  is the width of the peak. The fits (solid lines in Fig. 8) yield the following values of the phenomenological parameters  $a$  and  $\Delta B$  for the three samples. For the underdoped sample (stars) at  $T=14$  K,  $a=7.26 \times 10^4$  G<sup>5/2</sup>,  $\Delta B=0.35$  T; for the optimally doped sample (circles) at  $T=12$  K,  $a=4.64 \times 10^4$  G<sup>5/2</sup>,  $\Delta B=0.45$  T, while for the overdoped sample (triangles) at  $T=16$  K,  $a=1.08 \times 10^4$  G<sup>5/2</sup>,  $\Delta B=0.21$  T.

Figure 9 shows the experimental phase transition lines  $B_{ST}(T)$  measured in the three  $LaSCO$  samples, underdoped (squares), optimally doped (stars) and the overdoped sample (rhombs). These lines exhibit a slightly concave shape with negative slope and approach  $B_{ST}(T_0)=0$  at a certain temperature  $T_0$ . While  $T_0$  is very close to  $T_c$  for the optimally doped and overdoped samples, it is significantly lower than  $T_c$  for the underdoped sample (see also Ref. 10). In order to compare these data with our theory we have to extend the theory to the whole temperature range up to  $T_c$ . We took into account thermal fluctuations on the microscopic scale phenomenologically by using the two-fluid model for the temperature dependence of the coherence length, and the penetration depth  $\xi^{-2}(t)=\xi_0^{-2}(1-t^4)$ ,  $\lambda^{-2}(t)=\lambda_0^{-2}(1-t^4)$ , where  $t=T/T_c$ . The transition line was described in the Sec. IV by a function  $b=g(b\tau)$  presented in Fig. 7 and fitted in Eq. (38) by a power function. Here the dimensionless parameters  $b$  and  $\tau$  were defined in Eq. (35) and Eq. (3) respectively. Both should be rescaled:

$$b(t) = (1 - t^4)s \left( \frac{\alpha t}{1 - t^4} \right) \simeq \left( s_1 \frac{(1 - t^4)^{\nu+1}}{t^\nu} - s_2 \frac{(1 - t^4)^\nu}{t^{\nu-1}} \right). \quad (40)$$

Fitting parameters are therefore the fourfold anisotropy parameter  $\eta$  and a material parameter  $\alpha = 16\pi^3\lambda_0^2 T_c / L_z \Phi_0^2$ . Using the measured values of the penetration length  $\lambda_0$ , coherence length  $\xi_0$  and the critical temperature  $T_c$  the fits yield  $\eta = 0.03$ ,  $\alpha = 10^{-4}$  for underdoped,  $\eta = 0.02$ ,  $\alpha = 10^{-4}$  for the optimally doped and  $\eta = 0.01$ ,  $\alpha = 8 \times 10^{-5}$  for the overdoped sample. The lengths of the stiff segments  $L_z$  is therefore of the order of  $10^{-4}$  cm which in turn implies that the tilt energy  $C_{44}/L_z^2 \sim C_{sq}/a_0^2$ . The results of this fitting procedure are shown as solid lines in Fig. 9 and demonstrate a very good agreement with the experimental data. Therefore, we thus conclude that the transition line location on the  $B$ - $T$  plane allows to determine the fourfold anisotropy parameter  $\eta$ . Note that  $\eta$  can also be determined independently from transport measurements. In particular, the flux flow resistivity, which is isotropic in the square vortex lattice phase, exhibits anisotropy in the rhombic phase. In the linear response  $J_i = \sigma_{ij} E_j$ , the fourfold symmetry implies that  $\sigma_{ij} = \delta_{ij} \sigma$  and therefore is rotationally invariant, while in the rhombic phase the remaining twofold symmetry is less restrictive:  $\sigma_{ij} = \delta_{ij} \sigma + \eta \sigma_{ij}^z$ ,  $\sigma_{11}^z = -\sigma_{22}^z = 1$ ,  $\sigma_{12}^z = \sigma_{21}^z = 0$ . The flux flow resistivity has been measured recently in *YBCO* single crystals.<sup>37</sup> However, even in the square lattice phase the anisotropy may show up beyond the linear response. Indeed the fourth rank nonlinear conductivity tensor  $\Delta J_i = \Delta \sigma_{ijkl} E_j E_k E_l$  already has a room for the second coefficient proportional to  $\eta$ , see Ref. 24.

## VI. DISCUSSION AND CONCLUSIONS

We first address the relation of the theory presented in this paper to other theories of the square-to-rhomb structural phase transition. The distinct general feature of our result is that the slope of the transition line is negative. There are three major approaches to the transition: the more basic is the microscopic approach starting with the BCS type theory (see Refs. 22 and 23), the second more phenomenological approach is based on the London approximation in which vortices appear as line-like objects (Kogan and collaborators<sup>20,28</sup> and the present theory belongs to this type), while the third, also a phenomenological approach, is based on the Ginzburg-Landau expansion near  $T_c$  (see Refs. 24, 25, and 27). The main result of the symmetry breaking, namely the slope of the SPT line, is in fact independent of the details of the theoretical approach. It rather reflects a more general property of the system: its symmetry. We start therefore the discussion with symmetry and entropy considerations.

In low  $T_c$  superconductors the slope of the rhomb-square<sup>12</sup> can be positive. This corresponds to a situation in which for a fixed magnetic field at low temperature the symmetric phase is stable, while upon heating two degenerate asymmetric ground states appear. Assuming that disorder can be neglected, this situation is unphysical. Quite generally, in statistical physics a symmetry breaking second order phase transition proceeds the other way around: from a

degenerate asymmetric (symmetry  $H$  lower than of Hamiltonian  $G$ ) vacuum to a symmetric one whose symmetry coincides with that of the Hamiltonian.<sup>38</sup> For example, upon increasing temperature ferromagnet becomes paramagnet, superconductor-normal metal, solid-liquid, etc. Although, to our knowledge, a rigorous proof does not exist, the reason for this is that upon heating excitations “across the energy barrier” separating the multiple symmetry broken ground states are generated and eventually the Gibbs state becomes symmetric and degeneracy disappears (the system regains ergodicity).

In vortex physics outside the domain of SPT this general rule holds. For example in very clean materials the melting line has a negative slope. Note that the phenomenon of inverse melting was observed in *BSCCO* (Ref. 1) and *YBCO* (Ref. 3) was shown to be caused solely by disorder for which the previous entropy argument does not apply.

In light of this, it is quite surprising to find out that many theoretical papers (which generally do not consider disorder) arrive at a conclusion that the square lattice upon heating becomes a less symmetric rhombic lattice. Therefore, in order to explain the positive slope of numerous structural phase transitions observed in low  $T_c$  materials (Refs. 12–14) one should explore other ideas. As noted above, disorder can provide such an explanation. In the presence of disorder the slope becomes positive as has been demonstrated in the case of the OD line.

To conclude, the unique temperature dependence of the phase transition line in *LaSCO* derived from the onset of the second magnetization peak, interpreted in the past as an order-disorder or decoupling transitions, was demonstrated to be consistent with being a structural phase transition in the vortex lattice.

## ACKNOWLEDGMENTS

We are grateful to E. M. Forgan, R. P. Huebener, and T. J. Yang for discussions. This work was supported by The Israel Science Foundation, ESF Program “Cosmology in the Laboratory,” and by the Heinrich Hertz Minerva Center for High Temperature Superconductivity. Y.Y. acknowledges support of the Israel Science Foundation Excellence Center Program. We are also grateful to the Binational Israel-USA and Germany-Israel Foundations for support and to the Inter-University Computational Center for providing CRAY J932 supercomputer facilities. B.R. acknowledges support of Albert Einstein Minerva Center for Theoretical Physics in Weizmann Institute and NSC grant of ROC92-2112-M009-024 and the hospitality of Bar Ilan University.

## APPENDIX

Coefficients of the quadratic Eq. (30) and quartic, Eq. (34) to the Gaussian free energy for any fourfold symmetric potential  $w(q_x, q_y)$  are

$$v_1 = \sum_{\mathbf{G}} G_y^2 w''_{xx}; \quad v_2 = \sum_{\mathbf{G}} (2w + 4G_x w'_x + G_x^2 w''_{xx}),$$

$$v_3 = - \sum_{\mathbf{G}} (2w + 4G_x w'_x + G_x G_y w''_{xy}), \quad (41)$$

$$v_{11} = \sum_{\mathbf{G}} \left( 2w + 8G_x w'_x + 2G_x^2 w''_{xx} + 8G_x G_y w''_{xy} + 4G_x^2 G_y w'''_{xxy} \right. \\ \left. + \frac{1}{2} G_y^4 w''''_{xxxx} + \frac{1}{2} G_x^2 G_y^2 w''''_{xxyy} \right),$$

$$v_{22} = \sum_{\mathbf{G}} \left( 14w + 56G_x w'_x + 38G_x^2 w''_{xx} + 8G_x G_y w''_{xy} + 4G_x^2 G_y w'''_{xxy} \right. \\ \left. + 8G_x^3 w''''_{xxx} + \frac{1}{2} G_x^4 w''''_{xxxx} + \frac{1}{2} G_x^2 G_y^2 w''''_{xxyy} \right),$$

$$v_{33} = \sum_{\mathbf{G}} \left( 16w + 64G_x w'_x + 16G_x^2 w''_{xx} + 64G_x G_y w''_{xy} \right. \\ \left. + 32G_x^2 G_y w'''_{xxy} + 4G_x^2 G_y^2 w''''_{xxyy} \right),$$

$$v_{21} = \sum_{\mathbf{G}} \left( 12G_y^2 w''_{xx} + 4G_x G_y^2 w''''_{xxx} + 4G_y^3 w''''_{xxy} + \frac{1}{2} G_x^4 w''''_{xxyy} \right. \\ \left. + \frac{1}{2} G_x^2 G_y^2 w''''_{xxxx} \right),$$

$$v_{23} = - \sum_{\mathbf{G}} \left( 12w + 48G_x w'_x + 18G_x^2 w''_{xx} + 36G_x G_y w''_{xy} \right. \\ \left. + 2G_x^3 w''''_{xxx} + 2G_y^3 w''''_{xxy} + 18G_x^2 G_y w''''_{xxy} + 2G_x^3 G_y w''''_{xxyy} \right),$$

$$v_{13} = - \sum_{\mathbf{G}} \left( 18G_y^2 w''_{xx} + 6G_x G_y^2 w''''_{xxx} + 6G_x^2 G_y w''''_{xxy} \right. \\ \left. + 2G_x G_y^3 w''''_{xxyy} \right), \quad (42)$$

respectively.

The sum is over reciprocal square lattice  $\mathbf{G}$  (Fig. 1), while derivatives are performed with respect to  $q_x, q_y$  at the reciprocal lattice points.

\*National Chiao Tung University, Department of Electrophysics, Hsinchu, Taiwan, R.O.C.

†Author to whom correspondence should be addressed.

<sup>1</sup>E. Zeldov, D. Majer, M. Konczykowski, V. B. Geshkenbein, V. M. Vinokur, and H. Shtrikman, *Nature (London)* **375**, 373 (1995); R. Liang, D. A. Bonn, and W. N. Hardy, *Phys. Rev. Lett.* **76**, 835 (1996); A. Schilling, R. A. Fisher, N. E. Phillips, U. Welp, D. Dasgupta, W. K. Kwok, and G. W. Crabtree, *Nature (London)* **382**, 791 (1996); M. Roulin, A. Junod, and E. Walker, *Science* **273**, 1210 (1996); S. P. Brown, D. Charalambous, E. C. Jones, E. M. Forgan, P. G. Kealey, A. Erb, and J. Kohlbrecher, *Phys. Rev. Lett.* **92**, 067004 (2004).

<sup>2</sup>F. Bouquet, C. Marcenat, E. Steep, R. Calemczuk, W. K. Kwok, U. Welp, G. W. Crabtree, R. A. Fisher, N. E. Phillips, and A. Schilling, *Nature (London)* **411**, 448 (2001).

<sup>3</sup>N. Kobayashi, T. Nishizaki, K. Shibata, T. Sato, M. Maki, and T. Sasaki, *Physica C* **362**, 121 (2001); K. Shibata, T. Nishizaki, T. Sasaki, and N. Kobayashi, *Phys. Rev. B* **66**, 214518 (2002).

<sup>4</sup>N. Avraham, B. Khaykovich, Y. Myasoedov, M. Rappaport, H. Shtrikman, D. E. Feldman, T. Tamegai, P. H. Kes, M. Li, M. Konczykowski, K. van der Beek, and E. Zeldov, *Nature (London)* **411**, 451 (2001).

<sup>5</sup>Y. Radzyner, A. Shaulov, and Y. Yeshurun, *Phys. Rev. B* **65**, 100513(R) (2002).

<sup>6</sup>D. Pal, S. Ramakrishnan, A. K. Grover, D. Dasgupta, and B. K. Sarma, *Phys. Rev. B* **63**, 132505 (2001); D. Pal, S. Ramakrishnan, and A. K. Grover, *Phys. Rev. B* **65**, 096502 (2002).

<sup>7</sup>D. Li and B. Rosenstein, *Phys. Rev. Lett.* **90**, 167004 (2003).

<sup>8</sup>T. Sasagawa, Y. Togawa, J. Shimoyama, A. Kapitulnik, K. Kitazawa, and K. Kishio, *Phys. Rev. B* **61**, 1610 (2000).

<sup>9</sup>Y. Radzyner, A. Shaulov, Y. Yeshurun, I. Felner, K. Kishio, and J. Shimoyama, *Phys. Rev. B* **65**, 100503(R) (2002).

<sup>10</sup>U. Divakar, A. J. Drew, S. L. Lee, R. Gilardi, J. Mesot, F. Y. Ogrin, D. Charalambous, E. M. Forgan, G. I. Menon, N. Momono, M. Oda, C. D. Dewhurst, and C. Baines, *Phys. Rev. Lett.* **92**, 237004 (2004).

<sup>11</sup>D. McK. Paul, C. V. Tomy, C. M. Aegerter, R. Cubitt, S. H.

Lloyd, E. M. Forgan, S. L. Lee, and M. Yethiraj, *Phys. Rev. Lett.* **80**, 1517 (1998).

<sup>12</sup>M. R. Eskildsen, A. B. Abrahamsen, V. G. Kogan, P. L. Gammel, K. Mortensen, N. H. Andersen, and P. C. Canfield, *Phys. Rev. Lett.* **86**, 5148 (2001).

<sup>13</sup>L. Ya. Vinnikov, T. L. Barkov, P. C. Canfield, S. L. Bud'ko, and V. G. Kogan, *Phys. Rev. B* **64**, 024504 (2001); L. Ya. Vinnikov, T. L. Barkov, P. C. Canfield, S. L. Bud'ko, J. E. Ostenson, F. D. Laabs, and V. G. Kogan, *Phys. Rev. B* **64**, 220508(R) (2001).

<sup>14</sup>T. Forgan (private communication).

<sup>15</sup>C. E. Sosolik, J. A. Stroschio, M. D. Stiles, E. W. Hudson, S. R. Blankenship, A. P. Fein, and R. J. Celotta, *Phys. Rev. B* **68**, 140503(R) (2003).

<sup>16</sup>B. Keimer, W. Y. Shih, R. W. Erwin, J. W. Lynn, F. Dogan, and I. A. Aksay, *Phys. Rev. Lett.* **73**, 3459 (1994); I. Maggio-Aprile, Ch. Renner, A. Erb, E. Walker, and O. Fischer, *Phys. Rev. Lett.* **75**, 2754 (1995).

<sup>17</sup>H. F. Hess, R. B. Robinson, R. C. Dynes, J. M. Valles, Jr., and J. V. Waszczak, *Phys. Rev. Lett.* **62**, 214 (1989); R. Gilardi, J. Mesot, S. P. Brown, E. M. Forgan, A. Drew, S. L. Lee, R. Cubitt, C. D. Dewhurst, T. Uefuji, and K. Yamada, *Phys. Rev. Lett.* **93**, 217001 (2004).

<sup>18</sup>R. Gilardi, J. Mesot, A. Drew, U. Divakar, S. L. Lee, E. M. Forgan, O. Zaharko, K. Conder, V. K. Aswal, C. D. Dewhurst, R. Cubitt, N. Momono, and M. Oda, *Phys. Rev. Lett.* **88**, 217003 (2002).

<sup>19</sup>B. Rosenstein and A. Knigavko, *Phys. Rev. Lett.* **83**, 844 (1999).

<sup>20</sup>V. G. Kogan, A. Gurevich, J. H. Cho, D. C. Johnston, M. Xu, J. R. Thompson, and A. Martynovich, *Phys. Rev. B* **54**, 12386 (1996); V. G. Kogan, M. Bullock, B. Harmon, P. Miranovic, Lj. Dobrosavljevic-Grujic, P. L. Gammel, and D. J. Bishop, *Phys. Rev. B* **55**, R8693 (1997); P. Miranovic and V. G. Kogan, *Phys. Rev. Lett.* **87**, 137002 (2001).

<sup>21</sup>K. Takanaoka, *Prog. Theor. Phys.* **46**, 1301 (1971).

<sup>22</sup>H. Won and K. Maki, *Phys. Rev. B* **53**, 5927 (1996).

<sup>23</sup>N. Nakai, P. Miranovic, M. Ichioka, and K. Machida, *Phys. Rev. Lett.* **89**, 237004 (2002).

- <sup>24</sup>D. Chang, C.-Y. Mou, B. Rosenstein, and C. L. Wu, Phys. Rev. Lett. **80**, 145 (1998); Phys. Rev. B **57**, 7955 (1998).
- <sup>25</sup>K. Park and D. A. Huse, Phys. Rev. B **58**, 9427 (1998).
- <sup>26</sup>V. D. Ashkenazy, G. Jung, and B. Ya. Shapiro, Phys. Rev. B **51**, 9052 (1995).
- <sup>27</sup>A. D. Klironomos and A. T. Dorsey, Phys. Rev. Lett. **91**, 097002 (2003).
- <sup>28</sup>A. Gurevich and V. G. Kogan, Phys. Rev. Lett. **87**, 177009 (2001).
- <sup>29</sup>P. M. Platzman and H. Fukuyama, Phys. Rev. B **10**, 3150 (1974).
- <sup>30</sup>M. J. W. Dodgson, V. B. Geshkenbein, H. Nordborg, and G. Blatter, Phys. Rev. B **57**, 14498 (1998).
- <sup>31</sup>T. Kimura, K. Kishio, T. Kobayashi, Y. Nakayama, N. Motohira, K. Kitazawa, and K. Yamafuji, Physica C **192**, 247 (2002).
- <sup>32</sup>C. P. Bean, Rev. Mod. Phys. **36**, 31 (1964).
- <sup>33</sup>M. C. Dai and T. J. Yang, Physica C **305**, 301 (1998).
- <sup>34</sup>E. H. Brandt, J. Low Temp. Phys. **26**, 709–735 (1977); Phys. Rev. B **34**, 6514 (1986).
- <sup>35</sup>E. H. Brandt, Rep. Prog. Phys. **58**, 1465 (1995).
- <sup>36</sup>H. Kleinert, *Path Integrals in Quantum Mechanics, Statistics and Polymer Physics* (World Scientific Publishing Co., Singapore, 1995).
- <sup>37</sup>R. P. Huebener (private communication).
- <sup>38</sup>P. M. Chaikin and T. C. Lubensky, in *Principles of Condensed Matter Physics* (Cambridge University Press, Cambridge, UK, 1995), Sec. 3.6, p. 132. The statement is a well known book. L.D. Landau and E.M. Lifshitz states that “Although a great majority of phase transitions is from lower to higher symmetry upon increasing temperature there are exceptions.” As an exception ferroelectric (segnetoelectric) transition is mentioned. However the lower temperature segnetoelectric transition is not a symmetry breaking one. Indeed at zero temperature a ferroelectric has just one ground state in which each sublattice chooses its ground state.